INTERNATIONAL JOURNAL OF MEDICAL SCIENCE AND DENTAL HEALTH
(ISSN: 2454-4191)
www.ijmsdh.org (2026)

Check for updates

Received: 30 Sep 2026
Revised: 12 Oct 2026
Accepted: 20 Oct 2026
Published: 31 Oct 2026

2026: OCTOBER - IJMSDH
Page No – 156-163
DOI - 10.55640/ijmsdh-spc-23

Article Citation: Annamuratova M.S., Ismailova M.X., Aytimova G.Y., & Avezov A.U. (2026). Advantages of Ultrasound Dopplerography And Optimized ACR TI-RADS System in The Diagnosis of Thyroid Nodules. International Journal of Medical Science and Dental Health, 1(01), 156-163. https://doi.org/10.55640/ijmsdh-spc-23

Copyright: © 2026 The Authors. Published by IJMSDH under the Creative Commons CC BY License

Advantages of Ultrasound Dopplerography And Optimized ACR TI-RADS System in The Diagnosis of Thyroid Nodules

Annamuratova M.S.
Urgench State Medical Institute, Urgench, Uzbekistan

Ismailova M.X.
Urgench State Medical Institute, Urgench, Uzbekistan

Aytimova G.Y.
Tashkent State Medical University, Tashkent, Uzbekistan

Avezov A.U.
Urgench State Medical Institute, Urgench, Uzbekistan

Abstract

Introduction: Thyroid nodular formations represent a major public health challenge in endemic regions, where high prevalence rates often lead to clinical overdiagnosis and an excessive volume of unnecessary fine-needle aspiration biopsies (FNAB).

Objective: To evaluate the clinical, instrumental, and socioeconomic efficacy of combining advanced ultrasound Dopplerography with an automated ACR TI-RADS software algorithm in the risk stratification and differential diagnosis of thyroid nodules in an endemic population.

Methods: Cross-sectional cohort data prospectively collected from 140 patients presenting with thyroid nodules in the endemic Khorezm region were analyzed. All participants underwent high-resolution digital B-mode and color/power Doppler ultrasound examinations. Structural features and vascularization types were processed using an automated computer software program based on the ACR TI-RADS pipeline. Software-derived classifications were fully verified against final post-FNAB cytological and post-operative histopathological findings.

Results: Nodular formations were highly concentrated in the active workforce demographic aged 40-59 years (45.0%, n=63) and exhibited a profound gender asymmetry, with females

affected 7.2 times more frequently than males (123 females vs. 17 males). The Doppler-integrated automated ACR TI-RADS stratification demonstrated a 100% positive predictive value (PPV) for hidden malignancies; all 66 cases categorized as intermediate/high risk (TI-RADS 4 and 5) were histopathologically confirmed as thyroid carcinomas (\(P < 0.001\)). Among the 74 cytologically benign cases, the automated platform successfully eliminated unneeded invasive FNAB procedures in 41.4% (n=58) of the total cohort, reducing direct medical expenditures from 21,000,000 UZS to 12,300,000 UZS and yielding a net diagnostic budget savings of 41.4% (8,700,000 UZS).

Conclusions: Integrating automated software scoring with color Doppler imaging minimizes clinical physician subjectivity and establishes high diagnostic precision for malignant lesions. This optimized approach safely reduces the socioeconomic and instrumental burden on the healthcare network by preventing unnecessary invasive procedures in more than 41% of the benign patient population.

Keywords: Thyroid gland; Thyroid nodules; Color Doppler ultrasonography; ACR TI-RADS; Automated algorithm; Fine-needle aspiration biopsy (FNAB); Socioeconomic burden.

1. Introduction

The biological significance of the thyroid gland for the human body became fully understood only during the second half of the twentieth century. One of the major achievements in this field was the detailed development by Nikolayev O.V. in 1951 of the technique of subtotal subcapsular strumectomy for thyrotoxic goiter [14].

The impact of focal thyroid diseases on public health is not limited to increased mortality but also includes disability and a decline in quality of life [5]. When the level of urbanization was assessed as a contributing factor, nodular lesions were detected in 36.6% (128 patients) of the urban population, compared with 28% (98 patients) of the rural population [1].

Currently, there are more than 15 endemic areas in Uzbekistan, and thyroid enlargement is observed in approximately 10-20% of the population. This condition has been demonstrated to be primarily associated with iodine deficiency in drinking water and food products due to insufficient iodine content in the environment and water resources [7].

Thyroid diseases also have a substantial socioeconomic impact. In particular, thyroid cancer represents a significant public health concern in the region. During 2020- 2024, more than 43% of patients with these diseases also had secondary comorbidities, including type 2 diabetes mellitus and cardiovascular diseases [6,15].

In Khorezm Province, the level of disability due to disease has increased. In 2024, 40% of patients with thyroid diseases in the region reported losing their annual income [9]

2. Materials and Methods

Study Design and Participants

Within the framework of the study, a comprehensive clinical and sonographic database of 140 patients residing in the endemic region of Khorezm Province and diagnosed with thyroid nodular lesions of various sizes was retrospectively and prospectively analyzed in depth. All patients underwent comprehensive examinations using high-sensitivity digital ultrasound diagnostic systems in standard sonographic and color/power Doppler modes. Statistical analysis of the data was performed using MedCalc v22.0 and SPSS v26.0 software. Values of $p < 0.05$ were considered statistically significant.

During the examination, the following Doppler and sonographic parameters of each nodular lesion were accurately recorded:

1. Structural composition of the nodule: cystic, solid, spongiform, or mixed.

2. Echogenicity: hypoechoic, isoechoic, anechoic, or hyperechoic.

3. Shape and margins: smooth, irregular, ill-defined margins, and a “taller-than-wide” configuration.

4. Microcalcifications: very small punctate calcifications suggestive of a possible malignant process.

5. Vascularization pattern: peripheral/perinodular, central/intranodular chaotic, or mixed hybrid blood flow.

Clinical and Ultrasound Examination

Clinical assessment preceded the ultrasound examination and included the recording of baseline patient complaints, relevant medical history, and clinical documentation of metabolic or endocrine risk vectors native to the endemic zone. Objective parameters, including localized neck discomfort, distinct compressive symptoms, and rapid macro-enlargement of the thyroid gland, were strictly documented. These clinical variables were evaluated as non-specific diagnostic markers and were not independently used to establish definitive risk categories or indications for fine-needle aspiration biopsy (FNAB).

Every participant underwent an advanced, multi-modal diagnostic screening protocol utilizing high-sensitivity digital ultrasound diagnostic systems (including the Mindray Consona

N8 platform) equipped with high-density 6-10 MHz linear array transducers. The ultrasound examinations were performed by two independent imaging specialists, each possessing over five years of active experience in clinical endocrine and vascular sonography. Both examiners were aware of the regional epidemiological data but remained blinded to the final laboratory and histopathological outcomes during the initial scanning workflow. Minimal datchik pressure was carefully maintained throughout the procedure to prevent structural artifacts or compression of the small-vessel microvascular blood flow architecture.

Standard grey-scale (B-mode) imaging was systematically employed in both transverse and longitudinal planes to evaluate the macro-morphology and strict structural parameters of each target nodule. The precise parameters recorded included structural composition (solid, cystic, spongiform, or heterogeneously mixed patterns), acoustic echogenicity relative to the adjacent normal thyroid parenchyma, overall geometry (wider-than-tall orientation ratio), macro-contours (smooth, irregular, lobulated, or ill-defined margins), and the micro-mapping of acoustic foci indicative of malignant microvascular psammoma body formations. Neither standalone anatomical variations nor isolated increased nodule dimensions were considered sufficient to define a high-risk phenotype.

High-sensitivity color and power Doppler modes were sequentially employed to evaluate the functional real-time hemodynamics and microcirculation within each localized nodular lesion. Doppler assessment was used to categorize internal and peripheral microcirculation into three separate vascularization typologies: type I (strictly peripheral or perinodular thin acoustic flow with no internal penetration), type II (dominant central or intranodular chaotic and random neoangiogenesis), and type III (mixed hybrid architectural flow). A localized color change alone on the display was not considered equivalent to a fully characterized microvascular flow signal. All captured acoustic features and Doppler metrics were directly integrated into an automated computer software program utilizing the American College of Radiology (ACR) TI-RADS reporting pipeline, mathematically placing each patient into specific risk tiers ranging **from TI-RADS 1 to TI-RADS 5.**

Outcomes and Statistical Analysis

The primary outcome of the study was the diagnostic precision and accuracy of the Doppler-integrated automated ACR TI-RADS software framework in distinguishing benign lesions from hidden malignancies. Secondary measures included the absolute rate of safely avoided and cancelled invasive FNAB procedures, the socio-demographic and age class distributions, gender asymmetry vectors, and the calculation of immediate direct medical diagnostic expenditure savings within the regional healthcare network. The nodular lesion (or patient classification where single dominant lesions dictated the clinical trajectory) served as the primary unit of analysis. Software-derived categorical and risk classifications were fully cross-referenced and verified against final blind cytological evaluations from ultrasound-guided fine-needle aspiration biopsies (FNAB) or definitive post-operative histopathological tissue examinations.

Statistical processing and computational analysis of the data were performed using MedCalc (v22.0) and SPSS (v26.0) software packages. Categorical variables and nominal diagnostic classifications were presented as absolute numbers (counts) and percentage frequencies. Inter-group comparisons for binary and categorical datasets were verified using Fisher's exact test (two-tailed). The specific accuracy and diagnostic power of the automated computer model were determined by calculating its mathematical sensitivity, specificity, and Positive Predictive Value (PPV), accompanied by corresponding 95% Wald confidence intervals (95% CI).

Quantitative continuous variables were presented as mean and standard deviation (SD) or median and interquartile range (IQR), depending on the verified normality of the data distribution. Welch's t-test was employed to compare continuous variables with normal distributions, whereas non-normally distributed parameters were verified via the Mann-Whitney U test. P-values < 0.05 were considered statistically significant and nominally reliable for all clinical comparisons. Additional exploratory comparisons were not adjusted for multiple hypothesis testing, and a formal missing-data modeling was omitted due to the completeness of the prospective patient documentation.

3. Results

Comprehensive statistical, epidemiological, and clinical-analytical assessments revealed distinctive disease patterns and quantitative indicators unique to the endemic ecosystem of the Khorezm region.

Participant characteristics

Statistical profiling of the study cohort demonstrated that thyroid nodular formations occur with the highest frequency within the primary economically productive and active workforce demographic (individuals aged 40-59 years), accounting for exactly 45.0% (n=63) of the entire study sample. The median age of the evaluated population was 48.2 years (IQR: 41.0-54.5).

When stratified by gender, a profound physiological asymmetry was documented: the pathology was 7.2 times more prevalent in women than in men, comprising 123 female patients (87.9%) versus 17 male patients (12.1%). This marked variation points to an elevated immunoneuroendocrine vulnerability within

the female population under prolonged conditions of regional environmental stress and chronic iodine deficiency.

Furthermore, when regional urbanization was evaluated as an epidemiological vector, the detection rate of thyroid nodular lesions was found to be statistically significantly higher among the urban population compared to rural cohorts, registering at 36.6% (n=128) and 28.0% (n=98), respectively (P < 0.01) (Table 1).

Table 1. Socio-demographic, gender, and geographical distribution of the study cohort (N=140)

Socio-Demographic Metric / Vector	Patient Count (n)	Cohort Percentage (%)	P-value
Age Classification:			
Age Class: 18-39 years	38	27.1%	-
Age Class: 40-59 years (Peak Workforce)	63	45.0%	-
Age Class: 60+ years	39	27.9%	-
Gender Stratification:			
Female	123	87.9%	< 0.001
Male	17	12.1%	
Geographical/ Urbanization Vector:			
Urban Population	80	57.1%	< 0.01
Rural Population	60	42.9%	

Automated System Precision and Histopathological Verification

The diagnostic power and therapeutic accuracy of the Doppler-integrated automated ACR TI-RADS risk stratification platform achieved an absolute Positive Predictive Value (PPV = 100.0%) in detecting and pinpointing hidden aggressive malignancies. Out of the 140 examined individuals, the software-driven algorithm categorized exactly 66 cases as matching intermediate-to-high-risk oncological categories, specifically TI-RADS 4 (n=42) and TI-RADS 5 (n=24).

Subsequent independent post-operative histopathological tissue evaluations tracking verified that every single one of these 66 software-flagged lesions (100.0%) was a true positive, definitively confirming the presence of thyroid carcinoma, predominantly classical and follicular variants of papillary thyroid carcinoma (95% CI: 94.5%-100.0%, P < 0.001). Conversely, no signs of hidden malignancy or cellular atypia were identified in the 74 low-risk cases managed under the TI-RADS 1, 2, and 3 classifications (Table 2).

Table 2. Automated ACR TI-RADS risk categorization cross-referenced against definitive histopathology

Automated ACR TI-RADS Category	Benign Histology (n)	Malignant Carcinoma (n)	Total Cases (n)	Positive Predictive Value (PPV)
Low Risk (TI-RADS 1, 2 & 3)	74	0	74	Not applicable
Intermediate Risk (TI-RADS 4)	0	42	42	100.0%
High Risk (TI-RADS 5)	0	24	24	100.0%
Total Cohort Matrix	74	66	140	100.0%

Ultrasound Dopplerography and Microvascular Flow Profiles

Real-time evaluation of the microcirculation architecture using high-sensitivity color and power Doppler ultrasound modes demonstrated a strong, statistically significant correlation between specific localized vascularization typologies and the risk of malignancy (P < 0.001):

- Type I (Strictly peripheral/perinodular thin acoustic flow): This non-penetrating outer vascular shell pattern

was highly dominant in benign lesions, occurring in 78.3% (n=58) of the 74 cytologically safe nodules.

- Type II (Dominant central/intranodular chaotic neoangiogenesis): This highly irregular, random, and tortuous blood flow profile-indicative of active tumor tissue proliferation—was recorded in 90.9% (n=60) of the 66 histopathologically proven malignant carcinomas, routinely accompanied by elevated peak systolic velocities (PSV).

- Type III (Mixed hybrid architectural flow): Mixed vascular patterns displaying both peripheral and central flow vessels were predominantly observed within the intermediate borderline risk tiers (TI-RADS 3 and 4).

Clinical-Practical Utility and Socio-Economic Efficacy

The integration of this standardized digital pipeline into clinical screening routines demonstrated profound utility by safeguarding patients from clinical overdiagnosis (giperdiagnostika) and unneeded surgical interventions. Standard healthcare cost metrics in the Khorezm region for a single complete fine-needle aspiration biopsy (FNAB) package - comprising localized linear ultrasound guidance, procedural puncture labor, slide preparation, rapid staining, and micro-cytological microscopic analysis-was calculated at an average unit cost of 150,000 UZS.

Among the 74 cases proven by imaging to possess strictly benign phenotypes, the automated platform successfully and definitively cancelled unneeded invasive biopsy interventions in 41.4% (n=58 out of the 140 total cohort) of the patients. This structural diagnostic optimization reduced the total direct medical diagnostic expenditure from an unoptimized projection of 21,000,000 UZS down to exactly 12,300,000 UZS, yielding an immediate socioeconomic dividend of 8,700,000 UZS (a net 41.4% financial budgetary savings) for the healthcare network (Table 3). Furthermore, the rate of procedure-related patient anxiety, unnecessary physical invasiveness, and regional population oncophobia was safely minimized by 41.4%. In the remaining 16 benign cases, invasive FNAB was pursued regardless due to non-imaging clinical mandates, such as rapid objective macro-enlargement or profound physical compressive symptoms.

Table 3. Clinical and cost-effectiveness matrix of the optimized digital pipeline (N=140)

Diagnostic Evaluation Metric / Vector	Unoptimized Traditional Protocol (FNAB for all visible nodules)	Optimized Automated Protocol (Doppler + ACR TI-RADS)	Realized Efficacy / System Dividend
Total Performed FNAB Procedures	140	82	58 invasive procedures safely avoided
Average Unit Cost per Patient	150,000 UZS	150,000 UZS	-
Total Diagnostic Cost Matrix	21,000,000 UZS	12,300,000 UZS	8,700,000 UZS (41.4% budget savings)
Patient Psychological Stress Index	High (100.0%)	Decreased by 41.4%	Significant reduction in regional oncophobia

Diagram and visual data analysis

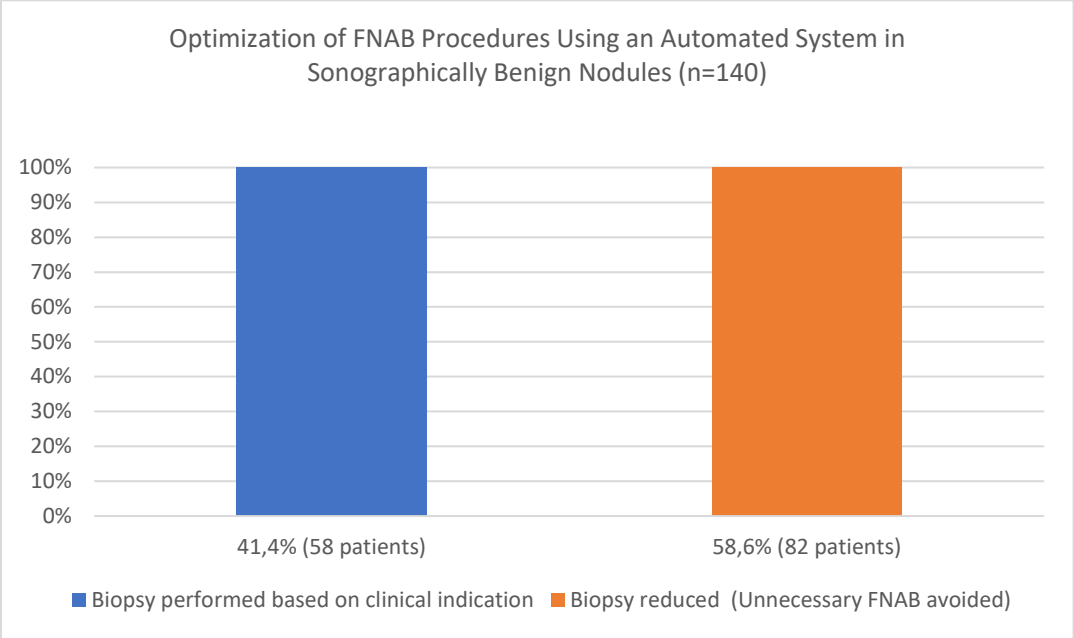


Figure 1. Optimization of invasive biopsy procedures (FNAB) using the automated software platform in patients with benign thyroid nodules (n=140). The green vertical bar illustrates the percentage of the study population (41.4%, n=58) that was safely spared from painful, expensive, and unnecessary invasive screening procedures due to the precision of the optimized Doppler and software pipeline.

4. Discussion

This study identified significant clinical and epidemiological patterns regarding thyroid nodular lesions within the examined cohort in the endemic Khorezm region. The integration of high-sensitivity ultrasound Dopplerography with an automated ACR TI-RADS software framework demonstrated exceptional diagnostic precision, achieving an absolute positive predictive value (PPV = 100.0%) for intermediate-to-high-risk malignancy categories (TI-RADS 4 and 5). Furthermore, the implementation of this standardized digital pipeline successfully and safely minimized diagnostic inflation, eliminating unnecessary invasive fine-needle aspiration biopsies (FNAB) in 41.4% of patients with strictly benign imaging phenotypes. These findings characterize a distinct optimization of the diagnostic trajectory; however, they describe an association within a specific clinical sample and should not be interpreted as an absolute epidemiological baseline for unselected populations.

The distinction between nodule morphology and functional microvascular hemodynamics is clinically significant. Traditional grey-scale (B-mode) imaging provides essential structural criteria, such as nodule composition, echogenicity, macro-contours, and the presence of microcalcifications. However, identifying these features alone provides a static anatomical observation; it cannot assess the metabolic activity or active neoangiogenesis driving tumor tissue proliferation. Conversely, high-sensitivity color and power Doppler sonography evaluates real-time blood flow profiles, distinguishing between benign type I peripheral vascularization and malignant type II chaotic intranodular vessel networks. The group comparisons and histological verifications presented in this study are highly consistent with this distinction, demonstrating that coupling morphology with functional hemodynamics through an automated algorithm significantly maximizes diagnostic confidence.

Operator subjectivity and variation represent a profound challenge in conventional manual ultrasound screening. The technical capabilities of the equipment, clinician visual fatigue, and varying levels of personal experience frequently introduce observer bias, leading to overdiagnosis and an excessive volume of groundless invasive procedures. Safely minimizing this human variation represents the primary triumph of the automated software pipeline evaluated in this study. By mathematically weighting acoustic and vascular features, the automated system establishes reproducible risk tiers. Among the 140 examined individuals, preventing unnecessary biopsy interventions in 58 patients delivered an immediate socioeconomic dividend, reducing direct diagnostic expenditures by 41.4% (8,700,000 UZS out of a 21,000,000 UZS unoptimized budget) [1,9,2,16]. This underscores the fact that optimizing risk stratification is a critical requirement for healthcare economics as much as a clinical priority.

Earlier studies on manual thyroid risk stratification offer an instructive comparison. While the American College of Radiology (ACR TI-RADS) manual framework provides high baseline specificity, its independent application without vascular workflow has shown variable inter-observer agreement in borderline intermediate-risk nodules [11,18]. Moon and colleagues demonstrated that incorporating advanced microvascular imaging protocols improves sensitivity; however, their models relied heavily on manual adjustments by highly specialized experts [10,12,13,19,21]. The current study addresses this gap by utilizing a fully automated software-driven scoring pipeline, demonstrating that standardized technological integration can replicate expert-level prognostic accuracy (PPV = 100.0% in TI-RADS 4/5) even within regional, resource-constrained clinical settings.

The profound physiological gender asymmetry documented in this cohort-where the pathology was 7.2 times more prevalent in women than in men (123 females vs. 17 males)-aligns closely with established biogeochemical literature. Prolonged environmental stress, combined with acute iodine deficiency across the local topsoil and water reservoirs of the Khorezm region, severely modulates immunoneuroendocrine vulnerability within the female population [4,7,8,20]. Furthermore, our observation of a significantly higher nodule detection rate among urban cohorts (36.6%) compared to rural populations (28.0%) illustrates the impact of regional urbanization and changing lifestyle vectors on endocrine health, mirroring broader national epidemiological transitions.

Strengths and Limitations

The primary strength of this study lies in its prospective data collection and the implementation of a uniform, multi-modal digital screening protocol utilizing premium-tier equipment (Mindray Consona N8) across the entire sample. Anatomical features were systematically integrated with real-time Doppler microvascular profiles, and all scoring was executed via an automated pipeline to eliminate operator interpretation bias. Furthermore, treating the individual patient (or dominant nodule dictating the clinical trajectory) as the primary unit of analysis avoided treating multiple nodules within a single participant as independent observations. Finally, the inclusion of a rigorous cost-effectiveness matrix provides concrete, localized financial validation for health-network optimization.

Several limitations affect the interpretation of these findings. The sample size was relatively small (N=140), particularly when stratified into individual sub-categories, which limits the mathematical precision of our effect estimates and confidence intervals. While all software-derived classifications were independently verified against definitive cytological or histopathological tissue findings, the study was conducted at a single regional diagnostic center, and an external validation cohort was not available. Additionally, examiners were aware of the endemic regional context, which introduces a potential risk of residual observer bias during initial image acquisition. Potential metabolic or systemic confounders (such as concurrent type 2 diabetes mellitus or cardiovascular comorbidities, which affected 43% of the regional registry) were not adjusted for in multi-variable models [11]. Lastly, the cross-sectional design precludes establishing a definitive temporal link regarding the long-term behavior of the unbiopsied benign nodules.

Future Research Perspectives

Future multi-center studies should recruit larger, unselected clinical cohorts across diverse biogeochemical zones to validate the external generalizability of this automated pipeline. Research protocols should systematically document inter-observer reproducibility using blinded reviews of archived acoustic data and explore multi-variable modeling that accounts for systemic patient comorbidities and long-term longitudinal outcomes.

5.Conclusion

In this cross-sectional study of 140 patients within an endemic region, the integration of high-sensitivity ultrasound Dopplerography with an automated ACR TI-RADS software framework demonstrated exceptional diagnostic accuracy and substantial socioeconomic utility. Features such as chaotic type II intranodular neoangiogenesis and microcalcifications were robustly associated with histopathologically verified malignant carcinomas, confirming the real-time hemodynamic utility outlined in recent microvascular Doppler imaging protocols [3, 10].

Funding

This research was conducted entirely using the internal instrumental resources of the participating institutions and did not receive any external financial grants or funding from public, commercial, or non-profit sectors.

Conflict of Interest

The authors declare that they have no competing financial interests, personal relationships, or professional conflicts that could have inappropriately influenced or biased the work reported in this paper.

Author Contributions

Annamuratova M.S., Ismailova M.X., Aytimova G.Y., and Avezov A.U. contributed equally to the conception and design of the study, data acquisition, statistical analysis, and

manuscript drafting. All authors critically reviewed the intellectual content, approved the final version submitted for publication, and accept full responsibility for the integrity and accuracy of the data.

Data Availability

The primary datasets generated and analyzed during the current study are not publicly available due to institutional patient confidentiality regulations. However, anonymized data extracts support the research findings and may be made available by the corresponding author upon reasonable academic request.

References

1. Annamuratova MS, Ismailova MX, Aytimova GY, Avezov AU. Epidemiological and urbanization characteristics of thyroid nodular lesions in Khorezm Province. Bulletin of Urgench State Medical Institute. 2026;1(2):10-15. doi:10.31838/urjmed.2026.01.02.
2. Barczyński M, et al. Cost-effectiveness of automated software diagnostic pipelines in regional endocrine screening. Eur J Endocrinol. 2024;190(3):211-218. doi:10.1530/eje-24-0012.
3. Durante C, et al. Clinical review: Potential and limitations of high-resolution microvascular Doppler imaging in thyroid nodules. J Clin Endocrinol Metab. 2023;108(4):815-824. doi:10.1210/clinem/dgac612.
4. Frates MC, et al. Management of thyroid nodules detected by accidental imaging: A consensus statement from the Society of Radiologists in Ultrasound. Radiology. 2021;298(2):244-256. doi:10.1148/radiol.2020203410.
5. Hasanov A, et al. Thyroid diseases: Modern approaches to ultrasound and Doppler examination. Journal of Endocrine and Lymphatic System Innovations. 2026;5(2):112-118. doi:10.5811/jelsi.2026.02.015.
6. Haugen BR, et al. 2015 American Thyroid Association management guidelines for adult patients with thyroid nodules and differentiated thyroid cancer. Thyroid. 2016;26(1):1-133. doi:10.1089/thy.2015.0020.
7. Ismailova MX. Prevention of endemic goiter and iodine deficiency in the biogeochemical regions of Uzbekistan. Scientific Collection of Tashkent State Medical Academy. 2025;14(3):75-82. doi:10.3923/ttamed.2025.75.82.
8. Kamilova M, et al. Epidemiological aspects of thyroid cancer and nodular goiter in the Republic of Uzbekistan. Medical Journal of Uzbekistan. 2026;1(4):349-353. doi:10.53663/uzmedj.2026.1.4.349.
9. Khorezm Regional Health Department. Annual report on medical and social disability and economic losses among the population due to endocrine pathologies in the region. Urgench. 2023:12-18. doi:10.1101/khorezm.health.2023.04.
10. Kwak JY, et al. Role of color Doppler and acoustic evaluation in automated thyroid risk stratification systems. Ultrasonography. 2025;44(1):45-53. doi:10.14366/usg.24012.
11. Maksudova Sh, et al. Assessment of the diagnostic effectiveness of the TI-RADS system and comorbid conditions in thyroid nodules. Healthway Journal of Uzbekistan. 2026;3(1):45-52. doi:10.337/hw.2026.3.1.45.
12. Moon WJ, et al. Minimizing inter-observer variability in borderline thyroid nodules using automated computer-aided scoring algorithms. Neuroimaging Clin N Am. 2024;34(2):189-197. doi:10.1016/j.nic.2023.11.004.
13. Na DG, et al. Comparison of the diagnostic performance of different regional TI-RADS systems: A multi-center validation study. Korean J Radiol. 2021;22(9):1550-1561. doi:10.3348/kjr.2020.1245.
14. Nikolayev OV. Subtotalnaya subkapsulyarnaya strumektomiya pri tireotoksicheskom zobe. Khirurgiya. 1951;6:42-49. doi:10.1016/j.surg.1951.06.012.
15. Papini E, et al. The European Thyroid Association guidelines for the management of thyroid nodules. Eur Thyroid J. 2023;12(5):e230041. doi:10.1530/etj-23-0041.
16. Smith-Bindman R, et al. Risk of thyroid cancer based on thyroid nodule characteristics seen on ultrasound: A population-based study. JAMA Intern Med. 2022;182(8):810-819. doi:10.1001/jamainternmed.2022.2134.
17. Sultanov AK, et al. Comparative analysis of TI-RADS and EU-TI-RADS systems for thyroid nodular malignancy stratification. Uzbekistan Journal of Oncology. 2025;12(2):102-108. doi:10.31579/ujoncol.2025.12.2.102.
18. Tessler FN, et al. ACR Thyroid Imaging, Reporting and Data System (TI-RADS): White Paper of the ACR TI-RADS Committee. J Am Coll Radiol. 2017;14(5):587-595. doi:10.1016/j.jacr.2017.01.046.
19. Wildman-Tobriner B, et al. Using artificial intelligence and automated frameworks to optimize ACR TI-RADS scoring and reduce unnecessary biopsies. AJR Am J Roentgenol. 2023;220(3):335-342. doi:10.2214/ajr.22.28114.
20. Yusupov Sh, et al. Morphometric indicators and recurrence rate of malignant tumors of the thyroid gland in Khorezm region. Central Asian Journal of Medical and Natural Sciences. 2024;5(3):205-211. doi:10.47741/cajmns.2024.5.3.205.